



# SANS-II at SINQ: installation of the former Risø-SANS facility

P. Strunz<sup>a,\*</sup>, K. Mortensen<sup>b</sup>, S. Janssen<sup>a</sup>

<sup>a</sup>Laboratory for Neutron Scattering, PSI and ETH Zürich, 5232 Villigen, Switzerland

<sup>b</sup>Risø National Laboratory, DK-4000 Roskilde, Denmark

## Abstract

SANS-II facility at SINQ (Paul Scherrer Institute)—the reinstalled former Risø small-angle neutron scattering instrument—is presented. Its operational characteristics are listed. Approaches for precise determination of wavelength, detector dead time and attenuation factors are described as well.

© 2004 Elsevier B.V. All rights reserved.

PACS: 61.12.Ex; 07.85.Jy; 83.85.Hf

Keywords: Small-angle neutron scattering; Neutron scattering instrumentation; Neutron wavelength; Raw-data treatment

## 1. Introduction

In May 2002, the SANS-II facility (the former Risø small-angle neutron scattering instrument) was installed at the Swiss Spallation Neutron Source SINQ (PSI) [1] in the framework of the PSI–Risø cooperation. The instrument is available for external users since September 2002. According to the agreement between PSI and Risø National Laboratory, half of the SANS-II beamtime is reserved for the Danish user community whereas the second half is scheduled via the SINQ proposal system.

The instrument can be used for SANS investigation of microstructures (polymer research, materials science, biology) in the size range 10–1000 Å. The aim of this paper is to inform about the

facility, its characteristics and about the wavelength calibration as well as simultaneous determination of the detector dead time and attenuation factors.

## 2. Basic parameters

The basic characteristics of SANS-II facility [2] at SINQ can be found in Fig. 1. The facility was upgraded by a new mechanical velocity selector (Astrium Space) which enables to select neutron wavelength in the range  $\lambda = 4.5\text{--}20\text{ Å}$ . Accessible  $Q$ -range is  $0.002\text{--}0.3\text{ Å}^{-1}$ .

As standard sample environment, a 7-position sample exchanger (with temperature control in the range 5–95°C), or a 2-position furnace (up to 300°C) can be employed. This equipment is installed in a sample chamber, which can be evacuated and connected to the

\*Corresponding author. Tel.: +41-56-310-5988; fax: +41-56-310-2939.

E-mail address: [pavel.strunz@psi.ch](mailto:pavel.strunz@psi.ch) (P. Strunz).

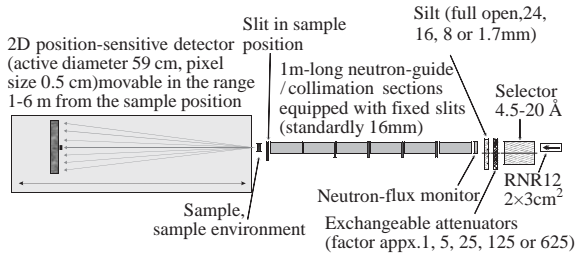


Fig. 1. SANS-II layout at PSI (at cold neutron guide RNR-12).

collimator and the detector tank without any additional windows.

A rotation or a translation table can be installed as well. This option enables the use of bulky and heavy equipment such as cryomagnet or a shear device. Sample environment available at SINQ is gradually integrated to SANS-II systems.

The instrument software is continuously developed as well. The instrument control program is being changed to the PSI standard–SICS. For the raw-data treatment, the following programs are available: BerSANS [3], Grasp [4], NOC [5], Risø software (author KM, not published).

### 3. Characterization of the instrument

A detailed characterization of the reinstalled instrument (flux measurement, relative PSD-pixel efficiency, wavelength calibration, dead time and attenuation factors) was carried out.

The flux in the sample position was measured by means of 2D position-sensitive detector (PSD) as well as by an independent detector, which provided also information about the  $\lambda$ -dependence of PSD efficiency. The typical determined flux normalized to the solid angle of the collimator aperture is 37 000 resp. 2500 neutrons/s/cm<sup>2</sup>/mrad<sup>2</sup> for  $\lambda = 4.5 \text{ \AA}$  resp.  $\lambda = 11.6 \text{ \AA}$  (measured with 4 m collimation). When comparing with SANS-I at SINQ, the flux for identical resolution is at SANS-II equal to 70% of that at SANS-I.

Calibration of the SANS measurements to the absolute scale using the SANS facility attenuator instead of a standard sample (e.g. water) is possible when the attenuation factor is known (see also Section 3.2). This possibility is, however,

conditional on the knowledge of the relative efficiency of individual pixels [5]. Such an efficiency map was measured and is available for the raw-data treatment.

#### 3.1. Wavelength calibration

The mean neutron wavelength depends on the tilt of the selector and can be calculated only approximately from its rotation speed without knowledge of the absolute selector tilt angle. Moreover, the neutron spectrum strongly decreases with increasing  $\lambda$ , thus deforming the relatively broad spectrum transmitted by the selector (the usual  $\Delta\lambda/\lambda$  is 10%). Therefore, the mean wavelength should be measured rather than theoretically calculated. For SANS facilities, it can be done using 001 Bragg reflection of silver behenate (AgBE) powder [6] which has large lattice spacing  $d_{001} = (58.378 \pm 0.008) \text{ \AA}$ . However, an uncertainty of the sample-to-detector distance  $L$  due to the PSD-active-volume thickness (4.5 cm) has to be taken into account. The mean path inside PSD in fact depends on its efficiency and hence  $L$  can be geometrically determined only with a precision of a few centimeters.

On the other hand, the distance between two positions of the PSD  $L_2 - L_1$  can be measured with a high accuracy, enabling thus a precise determination of the AgBE Bragg angle  $2\theta$  by measuring at two PSD distances:

$$\tan(2\theta) = (h_2 - h_1)/(L_2 - L_1). \quad (1)$$

Peak positions on PSD  $h_{1,2}$  (at  $L_{1,2}$ , relative to the center) are determined by fitting azimuthally averaged data by a Gaussian. With the knowledge of  $\theta$ , the actual mean wavelength along with the exact sample-to-detector distance can be evaluated:

$$\lambda = 2d_{001} \sin \theta \quad \text{and} \quad L_{1,2} = h_{1,2}/\tan(2\theta). \quad (2)$$

The mean neutron path in the active volume of the PSD was found to be 2 cm (for  $\lambda = 6.07 \text{ \AA}$ ). The obtained dependence of  $\lambda$  on the relative selector tilt is displayed in Fig. 2. The relative tilt angle was adjusted in such a way, that the resulting wavelength corresponds to that theoretically

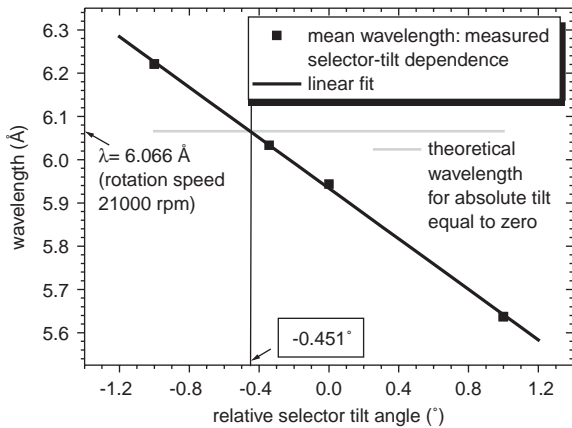


Fig. 2. Dependence of  $\lambda$  on the relative selector tilt for SANS-II.

calculated for the given speed of the non-tilted selector.

### 3.2. Dead time and attenuation factors

In case the investigated SANS sample exhibits large scattering intensity (as e.g. porous materials), corrections for dead time  $\tau$  of the PSD and its electronics are indispensable. For determination of  $\tau$ , a calibrated attenuator can be employed (e.g. the one integrated to the facility—Fig. 1). However, the precise determination of the attenuation factor  $A$  is to some extent influenced by the dead time and these two tasks should not be separated. The real non-attenuated intensity  $J_{R0}$  is connected with the real attenuated intensity  $J_{RA}$  by the relation  $J_{R0} = AJ_{RA}$ . The following relations can be thus written:

$$\begin{aligned}
 J_{R0} &= \frac{J_{M0}}{1 - \tau J_{M0}} - J_{Cd0} = AJ_{RA} \\
 &= A \left[ \frac{J_{MA}}{1 - \tau J_{MA}} - J_{CdA} \right], \quad (3)
 \end{aligned}$$

where  $J_{M0}$  is the intensity measured by PSD for the beam not attenuated by the facility attenuator and  $J_{MA}$  is the intensity measured for the beam attenuated by the facility attenuator. Under the same conditions, the background  $J_{Cd0}$ , resp.  $J_{CdA}$ , is additionally measured with the beam blocked by a piece of cadmium in the sample position. Eq. (3)

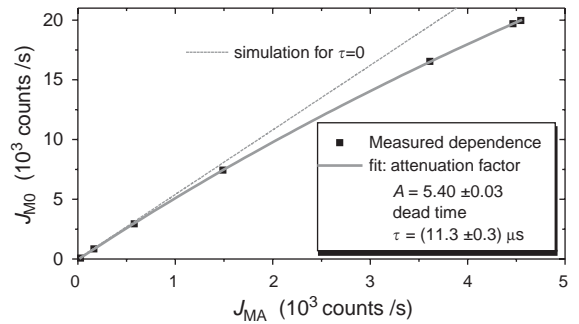


Fig. 3. Measured and fitted dependence of non-attenuated intensity on the attenuated one (facility attenuator No. 1). Both dead time  $\tau$  and attenuation factor  $A_1$  are determined by fit. Similarly, attenuating factors of the attenuator No. 2 ( $A_2 = 31.0 \pm 0.2$ ) and 3 ( $A_3 = 129.6 \pm 3.6$ ) were determined.

can be transformed to read

$$\begin{aligned}
 J_{M0} &= 1 / (\tau + \{A[(1/J_{MA} - \tau)^{-1} - J_{CdA}] \\
 &\quad + J_{Cd0}\}^{-1}). \quad (4)
 \end{aligned}$$

When  $J_{M0}$  is measured versus  $J_{MA}$ —i.e.  $J_{M0} = f(J_{MA})$ —the dependence can be fitted with the free parameters  $\tau$  and  $A$ . Spread of  $J_{M0}$  and  $J_{MA}$  values can be reached by measuring at varying wavelength. Alternatively, the slit size can be varied or the additional attenuator in the sample position can be exchanged (such attenuation is anyway necessary in order not to damage the PSD by the full primary beam as the beamstop is always removed). The result for the SANS-II PSD and attenuator 1 is displayed in Fig. 3.

## 4. Summary

SANS-II is currently in routine operation and fully characterized (some novel approaches are listed in this paper). Parallel to the characterization, altogether 13 experiments by groups from 11 different institutes were carried out on SANS-II in the period August–December 2002. They were mainly oriented to polymer science, but studies in other fields (materials science, biology) were performed as well.

The foreseen short-term improvements of the facility are: (i) new sample holder system (increase

of the beam cross-section), (ii) prolongation of the collimation system (background decrease), (iii) high-temperature furnace integration.

### Acknowledgements

The authors are grateful to S. Bang, F. Saxild, B. Breiting, J. Holm, C.G. Sorensen, O. Rasmussen, T. Kjaer (all Risø), P. Keller, C. Kägi, T. Mühlebach, R. Schneider, R. Thut, R. Bürge, G. Frey (all PSI) for the technical assistance during the installation. The authors thank J. Kohlbrecher

(PSI) for providing the AgBE sample and for modifications of BerSANS, as well as C. Dewhurst (ILL) for the Grasp upgrade.

### References

- [1] <http://sinq.web.psi.ch/>.
- [2] <http://sinq.web.psi.ch/sinq/instr/sans2.html>.
- [3] U. Keiderling, *Physica B* 234–236 (1997) 1111.
- [4] C. Dewhurst, [http://www.ill.fr/lss/grasp/grasp\\_main.html](http://www.ill.fr/lss/grasp/grasp_main.html).
- [5] P. Strunz, et al., *J. Appl. Crystallogr.* 33 (2000) 829.
- [6] R. Gilles, et al., *Mat. Sci. Forum* 321–324 (2000) 264.